Transactions of the Materials Research Society of Japan 33[3] 645-648 (2008)

Influence of surface roughness in depth profile analysis of the strain distribution in surface layer using x-ray diffraction at small glancing angles of incidence

Yoshikazu Fujii
Center for Supports to Research and Education Activities, Kobe University,
Rokkoudai-cho, Nada-ku, Kobe 657-8501
Fax: 81-78-803-6116, e-mail: fujiiyos@kobe-u.ac.jp

The intensity of x-ray propagation in surface layer materials characterized by a complex refractive index that changes continuously with depth was derived, and with use of the result, an analyzing method for evaluating the depth profiles of the strain distribution in the surface layer was studied. In this study, analyzing the incidence angle dependence of the scattered angles of diffracted x-rays from polycrystalline in surface layer with surface roughness, the depth profile of the strain in the surface layer is obtained. And, the influence of surface roughness in depth profile analysis of the strain distribution is studied.
Key words: x-ray diffraction at small glancing angles of incidence, depth profile, surface strain

1. INTRODUCTION

Knowing the residual stress of the surface layer becomes important on the surface where the alloy was plated for the strength improvement on the surface of the material. The residual stresses in poly-crystalline surface were measured using the glancing incidence x-ray diffraction technique.

In the previous studies, the in-depth distribution of residual stresses of the surface layer was estimated with the use of the term of penetration depth [1,2]. These estimations cannot be applied to the residual stress distribution analysis of the surface layer materials as multi thin films and compound plating layers with rough surface and rough interfaces because the densities of the surface layer materials change continuously in depth.

I therefore derived the x-ray intensity propagating during the surface layer materials of which density changes continuously in depth, and calculated the dependence of the diffracted x-ray intensity on the glancing angle. With the use of the analyzing method, the depth profiles of the strain distribution in the surface layer were studied [3,4].

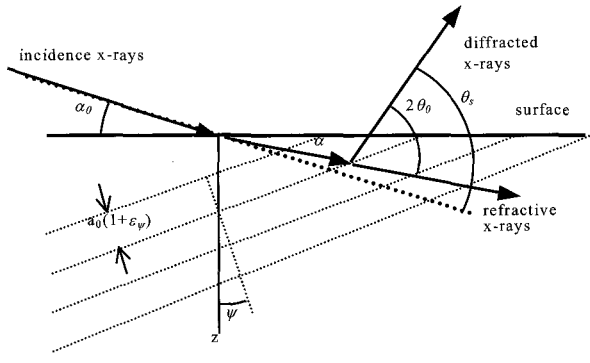

Fig. 1. The schematic of glancing incidence x-ray diffraction at angle α_0 of incidence.

The derived analyzing method can be applied to the strain distribution analysis of the surface layer materials of which densities change continuously in depth as the surface with roughness and layers structure. In this study, the influence of surface roughness in depth profile analysis of the strain distribution is discussed.

2. ANALYSIS

Figure 1 shows the schematic diagram of glancing incidence x-ray diffraction at small angle α_0 of incidence. The scattering plane is in xz-plane, x-axis is parallel to the surface, z-axis is normal to the surface. Scattered angle θ_s of the diffracted x-ray from the crystal plane with the strain in depth z is

$$\theta_s = 2\theta_0 - 2\varepsilon_\psi(z)\tan\theta_0 + \alpha_0 - \alpha(z) \quad , \quad (1)$$

where θ_0 is the Bragg angle at stress free, α_0 is the incidence angle, $\alpha(z)$ is the refracting angle and $\varepsilon_\psi(z)$ is strain in depth z in the direction normal to the diffraction plane that has inclined by ψ from the surface. Figure 1 shows the effect of refraction on the scattered angle θ_s at small glancing angle α_0, where the effect of refraction on x-ray exited from the surface is neglected.

In the condition of small glancing angle of incidence, most of the x-rays are scattered by only shallow regions near the surface. In the region, the stress σ_z in the direction z normal to the surface can be neglected, *i.e.* $\sigma_z = 0$. Here the isotropic stress, *i.e.* $\sigma_x = \sigma_y = \sigma$ is assumed, the strain ε_z is

$$\varepsilon_z = -\frac{2\nu}{E}\sigma \quad , \quad (2)$$

where ν is the Poisson's ratio and E is the Young's modulus.

On the stress estimation by using x-ray diffraction at small glancing angle incidence, $\sin^2\psi$ diagram method is useful, but it becomes difficult to apply the method due to its nonlinearity when a sample has stress gradient in the surface, *i.e.* the co-axial stress σ becomes $\sigma(z)$; the in-depth distribution of residual stresses. This difficulty

is due to the changing strain with depth dependence to the surface, *i.e.* the strain $\varepsilon_z = \varepsilon_z(z)$. The strain $\varepsilon_\psi(z)$ in the direction normal to the diffraction plane is related in $\varepsilon_z(z)$ as,

$$\varepsilon_\psi(z) = \varepsilon_z(z)\{1 - \frac{1+\nu}{2\nu}\sin^2\psi\}. \quad (3)$$

In the previous studies, the residual stresses $<\sigma>$ in the surface layer was estimated with the use of the term of penetration depth T as the following equation, [1,2]

$$<\sigma> = \frac{1}{T}\int_0^h \sigma(z)\exp(-z/T)dz \ , \quad (4)$$

where h is specimen thickness, the effect of refraction was neglected, *i.e.*, $\alpha(z)=\alpha_0$, and the penetration depth T was approximately shown as $\sin\alpha_0/\mu$, where μ is a linear absorption coefficient.

With using above relation, the residual stresses $<\sigma>$ in the previous studies was estimated as the following equation [1,2],

$$\theta_s = 2\theta_0 + 2\tan\theta_0(\frac{2\nu}{E} - \frac{1+\upsilon}{E}\sin^2\psi)\frac{1}{T}\int_0^h \sigma(z)\exp(-z/T)dz \ . \quad (5)$$

However, these estimations cannot be applied to the residual stress distribution analysis of the surface layer materials as compound plating layers with rough surface of which densities change in depth, because T is not constant in these materials.

We therefore characterized the refractive index of the surface layer materials with complex refractive index, which changes continuously in depth, and derived the x-ray intensity propagating during the surface layer materials.

The x-ray intensity propagating during the surface layer materials is derived first. The intensity of x-rays, *i.e.*, the electric and magnetic fields propagating in the material, can be obtained using Maxwell's equations [5].

The effects of x-rays on the material are characterized by complex refractive index n, which changes continuously with depth. The material for which the density changes continuously with depth is divided into thin layers with thickness d. The reflectance of multiplayer system can be calculated using the recursive formalism given by Parratt [6].

Let n_j be the refractive index of the j-th layer, defined as

$$n_j = 1 - \delta_j - i\beta_j \ , \quad (6)$$

where δ_j and β_j are the real and imaginary parts of the refractive index. These optical constants related to the atomic scattering factor and electron density of the j-th layer material. For x-rays of wavelength λ, the optical constants of the j-th layer material consisting of N_{ij} atoms per unit volume can be expressed as

$$\delta_j = \frac{\lambda^2 r_e}{2\pi}\sum_i f_{1i}N_{ij} \ , \quad \beta_j = \frac{\lambda^2 r_e}{2\pi}\sum_i f_{2i}N_{ij} \ , \quad (7)$$

where r_e is the classical electron radius and f_{1i} and f_{2i} are the real and imaginary parts of the atomic scattering factor of the i-th element atom, respectively.

The electric field of x-ray radiation at glancing angle of incidence α_0 is expressed as

$$\boldsymbol{E}_0(z) = \boldsymbol{A}_0\exp[\,i(\boldsymbol{k}_0\cdot\boldsymbol{r} - \omega t)\,] \ . \quad (8)$$

Incident radiation is usually decomposed into two geometries to simplify the analysis, one with incident electric field $\boldsymbol{E}$ parallel to the plane of incidence (p-polarization) and one with $\boldsymbol{E}$ perpendicular to that plane (s-polarization). An arbitrary incident wave can be represented in terms of these two polarizations. E_{0x} and E_{0z} are p-polarization, and E_{0y} is s-polarization, and those components of the amplitude's electric vector are expressed as

$$A_{0x} = -A_{0p}\sin\alpha_0 \ , \quad A_{0y} = A_{0s} \ , \quad A_{0z} = A_{0p}\cos\alpha_0 \ . \quad (9)$$

The components of wave vector of incidence x-rays are

$$k_{0x} = \frac{2\pi}{\lambda}\cos\alpha_0 \ , \quad k_{0y} = 0 \ , \quad k_{0z} = \frac{2\pi}{\lambda}\sin\alpha_0 \ . \quad (10)$$

The electric field of x-rays propagating in the j-th layer material is shown as

$$\boldsymbol{E}_j(z) = \boldsymbol{A}_j\exp[\,i(\boldsymbol{k}_j\cdot\boldsymbol{r} - k_{jz}(j-1)d - \omega t)\,] \ . \quad (11)$$

The amplitude $\boldsymbol{A}_j$ of j–th layer is derived from continuity equations for the interface between the j-1 and j layer as shown by

$$\boldsymbol{A}_1 = \boldsymbol{\Phi}_1\boldsymbol{A}_0 \ , \quad \boldsymbol{A}_j = \boldsymbol{\Phi}_j\boldsymbol{A}_{j-1}\exp(ik_{j-1,z}d) \ . \quad (12)$$

By the condition of incident x-ray, the z-direction component of wave vector of the j-th layer is shown as

$$k_{j,z} = \frac{2\pi}{\lambda}\sqrt{n_j^2 - \cos^2\alpha_0} = \frac{2\pi}{\lambda}(a_j + ib_j) \ . \quad (13)$$

The Fresnel coefficient tensor for refraction on the interface between $j-1$ and j layer is given by

$$\boldsymbol{\Phi}_{j,xx} = \frac{2n_{j-1}^2(a_j + ib_j)}{n_j^2(a_{j-1} + ib_{j-1}) + n_{j-1}^2(a_j + ib_j)}$$

$$\boldsymbol{\Phi}_{j,yy} = \frac{2(a_{j-1} + ib_{j-1})}{(a_{j-1} + ib_{j-1}) + (a_j + ib_j)}$$

$$\boldsymbol{\Phi}_{j,zz} = \frac{2n_{j-1}^2(a_{j-1} + ib_{j-1})}{n_j^2(a_{j-1} + ib_{j-1}) + n_{j-1}^2(a_j + ib_j)} \ . \quad (14)$$

Using these equations, the electric field of x-ray propagating in j-th layer is expressed as

$$\boldsymbol{E}_j(z) = (\prod_{J=1}^{j}\boldsymbol{\Phi}_J)\boldsymbol{A}_0\exp[\,i(k_{0x}x + d\sum_{J=1}^{j-1}k_{Jz} + k_{j,z}(z-(j-1)d) - \omega t)\,] \ , \quad (15)$$

where reflective x-ray in the interface in each layer is assumed to be small enough.

The intensity of the refractive x-ray in j-th layer at depth z is shown as

$$I(z) = (\prod_{J=1}^{j}\boldsymbol{\Phi}_J)\boldsymbol{A}_0\cdot(\prod_{J=1}^{j}\boldsymbol{\Phi}_J)\boldsymbol{A}_0\cdot\exp\{-d\frac{4\pi}{\lambda}\sum_{J=1}^{j-1}b_J - \frac{4\pi}{\lambda}b_j(z-(j-1)d)\} \ . \quad (16)$$

Here, it is assumed that the intensities of the x-rays diffracted from polycrystalline surface layer are in proportion to the sum of the refractive x-ray intensity in each layer of those polycrystalline, *i.e.*, x-rays scattered at different depth are assumed to be no interference, and the influence on x-ray intensity by interference in each crystal grain is disregarded.

Then the peak angle of the diffracted x-rays is shown in the following equation,

$$\theta_s(\alpha_0) = 2\theta_0 + \alpha_0 + \frac{\int_0^h[2\tan\theta_0(\frac{1+\nu}{2\nu}\sin^2\psi - 1)\varepsilon_Z(z) - \alpha(z)]I(z)dz}{\int_0^h I(z)dz} \ , \quad (17)$$

where $I(z)$, $\alpha(z)$ and $\varepsilon_\psi(z)$ are function of the incidence angle α_0, therefore θ_s is function of α_0.

The incidence angle dependence of the scattered angle $\theta_s(\alpha_0)$ of the diffracted x-rays can give good information to investigate the depth profile of the strain distribution in the surface layer materials of which densities change continuously in depth as the surface with roughness and layers structure.

3. DEPTH PROFILING OF STRAIN DISTRIBUTION UNDER ROUGH SURFACE

The strain distribution in the poly-crystalline surface layer of the chromium coating steel was investigated. Thickness of chromium layer was about 2 μm. The surface roughness of the specimen was about 100 nm (r.m.s) by measured with the stylus-type surface rough meter.

Intensities of the diffracted x-rays on the chromium coating steel were measured at various incidence angles with Synchrotron radiation at SPring-8 BL24XU [7].

The scattered angles of x-rays diffracted from Cr (310) by poly-crystalline chromium in the surface layer are shown in Fig. 2. The increase in the scattered angle θ_s at smaller incidence angle α_0 is due to the effect of refraction. Analyzing the incidence angle dependence of the diffraction angle, the depth profiles of the strain distribution in the surface layer can be derived.

At first, the incidence angle dependence of scattered angle was calculated with the constant strain ε_z. By comparison with calculated and observed scattering angle, the strain seems to decrease at smaller angle of incidence.

Next, the incidence angle dependence of scattered angle is calculated with the strain distribution in the surface layer of the chromium coating as the following equation model,

$$\varepsilon_z = -0.018\left\{1-\exp\left(-\frac{z}{r}\right)\right\}, \quad (18)$$

where the surface is assumed to be flat. Calculated results for several strain distribution is shown in Fig. 2. The calculation result of almost reproducing the experiment result can be obtained by putting a suitable parameter in the strain distribution model.

The experiment result is reproduced when assuming r=100 nm in eq. (18) of the strain distribution. However, it has not been considered yet that the surface is rough in this model.

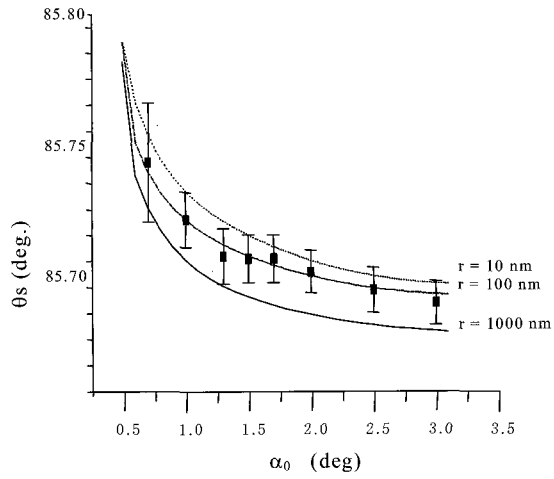

Fig. 2 Comparison between calculated and observed scattering angle. The square dots with error bar are experimental results. The lines are calculated results with several strain distribution models in the surface layer.

Then, the incidence angle dependence of scattered angle is calculated on rough surface, where the strain distribution range r is 100nm in eq. (18). The surface roughness is characterized with the root mean square deviation σ of the surface with respect to a flat surface. The density $\rho_M(z)$ of the polycrystalline chromium coating in the depth z with the surface roughness of σ is expressed as

$$\rho_M(z) = \int_{-\infty}^{z} \frac{1}{\sqrt{2\pi}\sigma} \exp\left(-\frac{x^2}{2\sigma^2}\right) dx \quad . \quad (19)$$

Then the effect of the surface roughness is reflected in the refractive index $n(z)$ and the intensity $I(z)$ of the refractive x-ray.

The estimation with using the term of penetration depth T in the research before cannot be applied to such material with the surface roughness since T depends on the incidence angle. The calculation for the depth profiling of the strain should be performed with using eq. (17).

Figure 3 shows calculated results of the incidence angle dependence on scattered angles for rough surfaces of several roughness of σ. It is understood that the scattered angle becomes small in the small angle 0.7~1.0 degree of incidence, when the surface roughness is large, and to deviate from the experimental results.

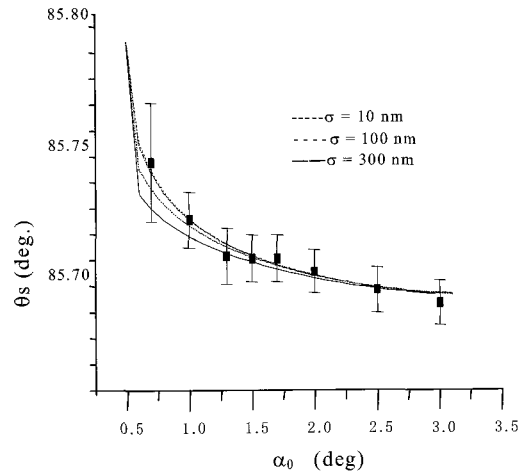

Fig. 3 Comparison between calculated and observed scattering angle. The lines are calculated results on rough surfaces of several roughness of σ, where the strain distribution range r is 100nm in eq.(18).

Therefore, when surface roughness exists, it is necessary to calculate in consideration both of the surface roughness and strain distribution. As the result of the calculation that simulates the observation, the strain distribution in the surface layer of the chromium coating is assumed as the following,

$$\varepsilon_z = -0.019\left\{1-\exp\left(-\frac{z}{80}\right)\right\} \quad (20)$$

where the surface roughness σ of 100 nm is considered in eq. (19).

Comparison between calculated and observed scattering angle of Cr(310) is shown in Fig. 4. The solid line is calculated result. The experiment result can be

reproduced by the fitting calculation with eyes guide, but the depth profile of the strain distribution in the surface poly-crystalline layers is different from the results of calculation in the case of flat surface. When it was not considered that the surface was rough, the obtained surface strain is estimated smaller than the value with the case to consider the surface rough.

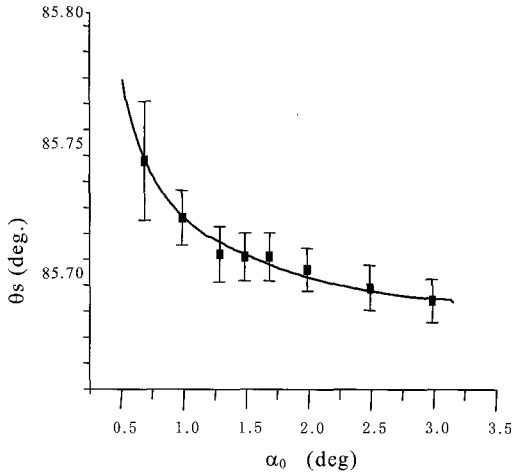

Fig. 4 Comparison between calculated and observed scattering angle. The solid line is a calculation result on rough surface with strain distribution, where the strain distribution range r is 80nm, and the surface roughness σ is 100 nm.

4. CONCLUSIONS

The x-ray intensities propagating during the surface layer materials of which density changes continuously in depth are derived, and analyzing the incidence angle dependence of the scattered angles of diffracted x-rays, the depth profile of the strain in the surface layer with surface rough is derived. When it was not considered that the surface was rough, the obtained surface strain indicated a different value with that of rough surface. It has been understood to have to consider the surface rough to analyze the surface strain distribution accurately.

REFERENCES

[1] P. Predecki et al, *Advances in X-ray Analysis* 36, 237 (1993).
[2] Y. Sakaida, S. Harada and K. Tanaka, *J. Soc. Mat. Sci. Japan* 42-477, 641 (1993).
[3] Y. Fujii, E. Yanase and K. Arai, *Applied surface Science*, 244, 230-234 (2005).
[4] Y. Fujii, E. Yanase and K. Nishio, *J. Phys.: Conf. Ser.*, 83, 012008 (2007).
[5] C. Slater and N. H. Frank, "Electromagnetism", McGraw-Hill, New York (1947).
[6] L. G. Parratt, *Phys. Rev.*, 95, 359 (1954).
[7] E. Yanase, K. V. Zolotarev, K. Nishio, Y. Kusumi, H. Okado and K. Arai, *J. Synchrotron Rad.*, 9, 309 (2002).

(Recieved December 10, 2007 ; Accepted March 29, 2008)